Available online at www.sciencedirect.com
SCIENCE DIRECT®
Chemical Physics Letters 372 (2003) 563–568
CHEMICAL PHYSICS LETTERS
www.elsevier.com/locate/cplett

Massive enhancement of persistent spectral hole-burning in the R-lines of $NaMgAl(oxalate)_3 \cdot 9H_2O$:Cr(III) by *partial* deuteration

Hans Riesen *, Joseph L. Hughes

School of Chemistry, University College, The University of New South Wales, ADFA, Canberra, ACT 2600, Australia

Received 3 March 2003; in final form 3 March 2003

Abstract

Partial deuteration of $NaMgAl(oxalate)_3 \cdot 9H_2O$:Cr(III) (0.5%) *increases* the quantum efficiency for persistent spectral hole-burning in the R_1-line by three orders of magnitude. A 50% deuterated crystal shows an impressive initial hole-burning efficiency of ≈0.1% and sharp anti-holes are observed in the range of ±15 GHz. A decrease of the quantum efficiency upon deuteration has often been reported in the literature and this has been rationalized on the basis of the lower tunnelling probability of the deuteron in the double well potential of hydrogen bonds. In contrast, the present findings of a sensational increase can be rationalized by a hole-burning mechanism based on 180° flip motions of the lattice water molecules around their pseudo C_2 axes. Considering the spin-flip nature of the electronic excitation this is an extraordinary finding. The deuteration effect may be used to design high-efficiency hole-burning materials for optical storage at liquid nitrogen temperatures.

1. Introduction

Non-photochemical spectral hole-burning is a ubiquitous phenomenon in amorphous systems: it is generally assigned to a variation of host-guest interactions in terms of the so-called two level systems (TLSs) model [1–3]. Due to their inherent structural order only a few crystalline systems have been reported to exhibit this effect [4–8].

We have recently reported the temperature dependence and magnetic field effects in persistent non-photochemical spectral hole-burning of the R-lines in $NaMgAl(oxalate)_3 \cdot 9H_2O$:Cr(III) [9–11]. We have shown that the temperature dependence of the homogeneous line width is governed by a direct process between the two ^2E levels and two-phonon Raman scattering by two pseudo-local vibrations [9]. Also, we have demonstrated that spectral holes in this system can be used as a *permanent* record of magnetic fields [11].

Early investigations of the crystal structure of $NaMgAl(oxalate)_3 \cdot 9H_2O$:Cr(III) indicated that the system crystallizes in either the $P3c1$ or $P\bar{3}c1$ space groups with six formula units per unit cell [12]. A more recent paper reported a refinement to $P\bar{3}c1$ with 10 water molecules of crystallization

* Corresponding author. Fax: +61-2-6268-80-17.
E-mail address: h.riesen@adfa.edu.au (H. Riesen).

0009-2614/03/$ - see front matter © 2003 Elsevier Science B.V. All rights reserved.
doi:10.1016/S0009-2614(03)00446-9

[13]. However, elementary analysis performed by several groups over the years has been in best agreement with nine water molecules [9]. A detailed knowledge of the hydrogen positions is important in order to understand the extraordinary hole-burning properties of this material. Hence we have revisited the crystal structure of $NaMgAl(oxalate)_3 \cdot 9H_2O$: the refinement establishes $P3c1$ as the space group with *nine* water molecules of crystallization [14]. All oxygen atoms of the oxalate ligands are involved in hydrogen bonding with water molecules. The six water molecules that are coordinated to magnesium(II) form one hydrogen bond each: three with an inner and three with an outer oxygen atom of the oxalate ligands. The remaining three water molecules are hydrogen bonded to the six water ligands of the magnesium(II) and each undergoes *two* hydrogen bonds to an inner and an outer oxygen atom of two separate oxalate ligands.

The present Letter reports on the massive effect of *partial* deuteration on spectral hole-burning properties, in particular the quantum efficiency. A mechanism based on 180° flip motions of the water molecules of crystallization is proposed.

2. Experiment

Samples of $NaMgAl(oxalate) \cdot 9H_2O$ and $NaMgCr(oxalate) \cdot 9H_2O$ were prepared as is described in the literature [15,16]. Mixed crystals containing 0.5% chromium(III) were grown by slow evaporation of solutions in D_2O/H_2O. The 'fully' deuterated $NaMgAl(oxalate) \cdot 9D_2O$:Cr(III) was prepared by twice freeze-drying 2 g of the material from ≈20 ml 99.9% D_2O. Crystals were then grown out of 99.9% D_2O in a desiccator. The crystals grow as relatively large (typical dimensions: $6 \times 1.5 \times 1.5$ mm) dichroic hexagonal prisms.

Excited state lifetimes were measured by modulating the light of an Ar^+ laser (Spectra Physics Stabilite 2017) by an acousto-optic modulator, and observing the luminescence at constant wavelength with the apparatus described below. For conventional transmission spectra the light of a 150-W halogen lamp was passed through a 694-nm interference filter with a 10-nm bandpass. The filtered light was then transmitted through the sample and analysed by a Spex 1404 monochromator, equipped with a 1200 grooves/mm holographic grating. The light was detected by a cooled RCA31034 photomultiplier and the signal was processed by a current-to-voltage preamplifier (Products-For-Research PSA) and a lock-in amplifier (EG&G 5210). Absorption spectra were calculated using an appropriate baseline.

Spectral holes were burnt and read out by a temperature and current stabilised diode laser (Thorlabs TEC2000 temperature controller with TCLDM9 thermoelectric mount, Thorlabs LDC500 laser current controller, Hitachi 6738MG laser diode). The line width of the laser was ~20 MHz as measured by a 300 MHz FSR confocal Fabry–Perot interferometer (Coherent model 240). The laser frequency was tuned by varying the injection current with a triangular waveform provided by a waveform generator (Stanford Research Systems SRS DS345). The frequency scans were calibrated by the Fabry–Perot etalon: a 1-mA increase in current results in a frequency shift of ca. −2.5 GHz. The laser light was measured in transmission by a Si photodetector (Thorlabs PDA55) before and after exposing the samples to laser light at constant wavelength. The signal was averaged on a digital storage oscilloscope (Tektronix TDS210) and subsequently on a Pentium III based PC. The samples were mounted on a sapphire window on the cold finger of a closed-cycle cryostat (Janis/Sumitomo SHI-4.5) by using heat conductive grease (Cry-con).

3. Results and discussion

Fig. 1 shows the effect of deuteration on the polarized absorption spectra of $NaMgAl(oxalate)_3 \cdot 9H_2O$:Cr(III) in the region of the $^2E \leftarrow {}^4A_2$ transitions. A shift to higher energy by ca. 3.5 cm^{-1} is observed for the deuterated sample. This shift is due to the variation of the difference of zero-point energies in the excited and ground states. In addition to the blue shift, a significant increase in the ^2E excited state lifetime from 0.89 to 2.94 ms occurs upon perdeuteration. Both effects indicate the presence of a sizeable vibrational

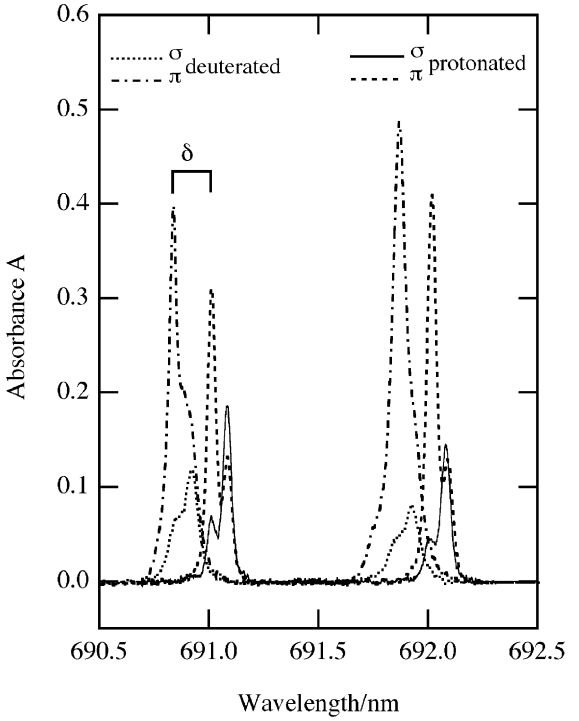

Fig. 1. Polarized absorption spectra at 2.5 K of a perprotonated and a fully deuterated crystal of NaMgAl(oxalate)$_3 \cdot 9H_2O$:Cr(III) 0.5%. Polarizations and the deuteration shift, δ, are indicated.

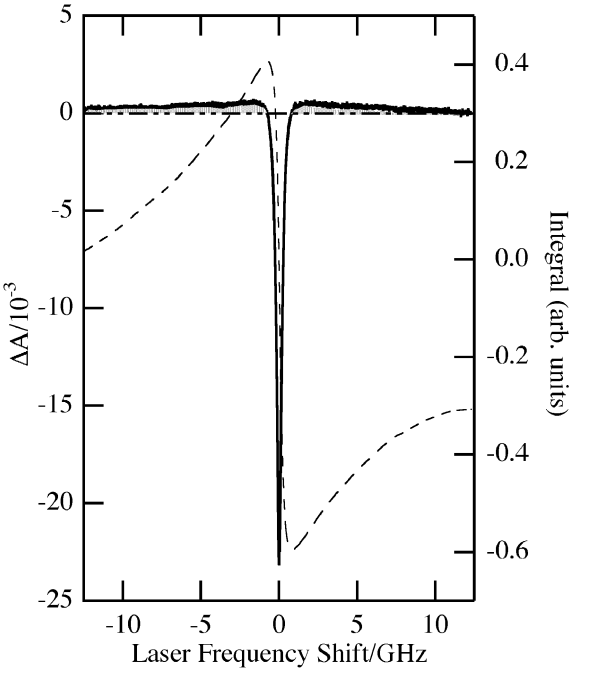

Fig. 2. Persistent spectral hole-burning in the R_1-line of perprotonated NaMgAl(oxalate)$_3 \cdot 9H_2O$:Cr(III) 0.5% at 2.5 K. The hole was burnt at 692.05 nm in σ polarization for 22 min with 1.5 mW of focussed laser light. The dashed line is the integral of the hole-burning spectrum and the shaded area indicates the 'photoproduct'.

coupling of the water molecules to the [Cr(oxalate)$_3$]$^{3-}$ complex: this coupling is facilitated by the hydrogen-bonds of the water molecules with the oxygen atoms of the oxalate ligands. We note here that crystals with a deuteration degree of ca. 50% display maxima of the R-lines between the perdeuterated and perprotonated transitions with a broader line width, reflecting the distribution of H_2O, HDO and D_2O species in the surroundings of [Cr(oxalate)$_3$]$^{3-}$. The lifetime of the ^2E excited state in the 50% deuterated sample is 1.48 ms.

Fig. 2 shows a spectral hole burnt into the R_1-line of perprotonated NaMgAl(oxalate)$_3 \cdot 9H_2O$:Cr(III) 0.5%. A focussed laser beam (irradiance $\approx$500 mW/cm^2) is required to burn relatively deep holes in a period of ca. 30 min. The shaded area in Fig. 2 indicates the 'photoproduct' which appears to be spread over a large fraction of the inhomogeneous width. The integral shows that most of the 'photoproduct' is accounted for in the scan range of $\pm$12 GHz, confirming the non-photochemical nature of the hole burning mechanism.

Fig. 3 displays hole-burning data obtained for partially deuterated NaMgAl(oxalate)$_3 \cdot 9H_2O$:Cr(III) 0.5% (50% deuteration degree). The hole-burning efficiency shows a *sensational increase* in comparison with the perprotonated sample, and a laser light irradiance of $\approx$3 mW/cm^2 is sufficient to burn very deep spectral holes within minutes. A striking feature is the appearance of sharp anti-holes with symmetric frequency shifts around the spectral hole of: $\pm$0.60, $\pm$0.90, $\pm$1.94, $\pm$2.54, $\pm$2.85, $\pm$4.28 (weak), $\pm$5.44 (weak), $\pm$6.32, $\pm$7.32, $\pm$9.39, $\pm$10.8, $\pm$14.3 and $\pm$14.9 GHz. Fig. 3b shows the hole-burning spectrum obtained by using an offset for the laser frequency during the burn period. In this graph the spectral hole is truncated in order to render the anti-holes more visible. The

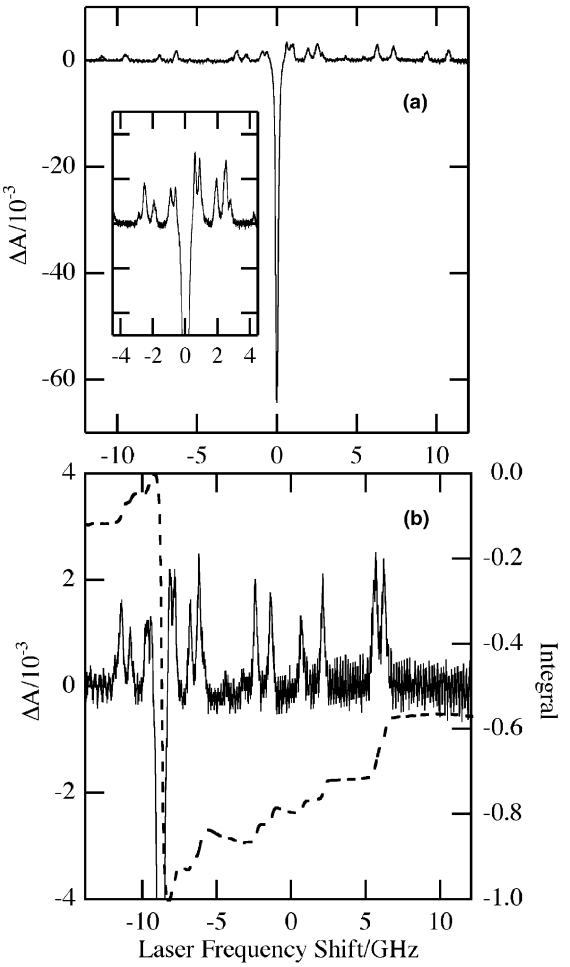

Fig. 3. Persistent spectral hole-burning in the R_1-line of partially deuterated (50% deuteration degree) NaMgAl(oxalate)$_3 \cdot 9H_2O$:Cr(III) 0.5% at 2.5 K. In panel (a) the hole was burnt for 10 min in σ polarization into the R_1 transition at 692.05 nm with an irradiance of ca. 3.5 mW/cm^2. The inset shows the anti-holes in the region of the hole (truncated). Panel (b) shows the anti-holes (hole is truncated) after the laser frequency was offset by −8.8 GHz in the burn period. The dashed line is the integral of the hole-burning spectrum.

integral establishes that the anti-holes on the higher energy side account for 50% of the hole area within the experimental accuracy. The same is true for the anti-holes on the lower energy side if a hole is burnt with an offset to higher frequency: thus the hole area is fully accounted for by the anti-holes. Some of the anti-holes are incredibly sharp with a width comparable to the spectral hole (100 MHz) for the relatively deep holes shown in Fig. 3. We note here that the 100-MHz hole-width contains a laser component of approximately 40 MHz.

Fig. 4 shows the hole-depths as a function of the burn time for the perprotonated and the partially deuterated (50%) systems with a laser light irradiance of 8 mW/cm^2. The inset shows the burn curve for the perprotonated sample using 1.5 mW of focussed laser light (≈660 mW/cm^2). We stress here that in both systems 100% deep holes can be burnt. The dashed lines in Fig. 4 are fits of single $(1 - e^{-\text{rate}\times\text{time}})$ and double exponentials for the perpotonated and 50% deuterated data, respectively. The need for a double exponential reflects a variation of hole-burning rates due to the distribution of HDO, H_2O and D_2O species.

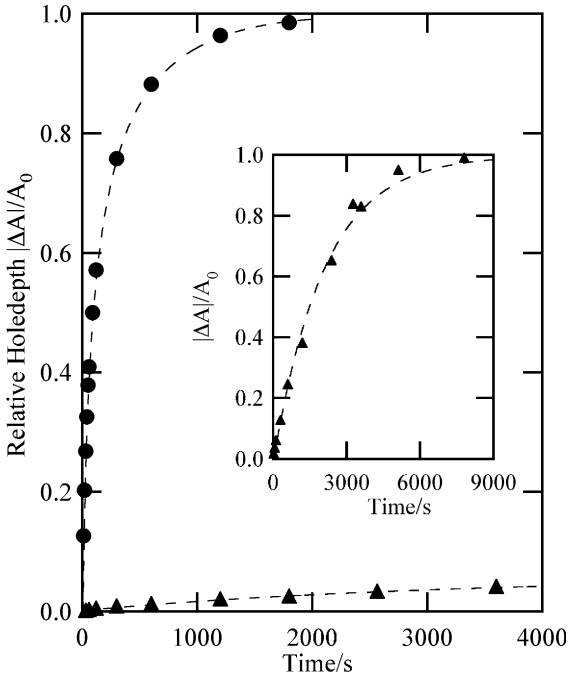

Fig. 4. Relative hole-depths in the R_1-line of perprotonated (solid triangles) and 50% deuterated (solid circles) NaMgAl(oxalate)$_3 \cdot 9H_2O$:Cr(III) 0.5% as a function of the burn time. Holes were burnt at 692.03 nm in π polarization with a laser irradiance of 8 mW/cm^2. The perprotonated and partially deuterated samples were 1.8 and 1.3 mm thick, respectively. The inset shows the relative hole-depth of the perprotonated crystal as a function of burn time with 1.5 mW of *focussed* laser light (≈660 mW/cm^2) at 692.05 nm.

The initial hole-burning efficiency ϕ can be calculated by using Eq. (1) where $c(\Gamma_h)$ is the concentration of centres (mol/cm^3) within one homogeneous line width, Γ_h, N_A is Avogadro's number, A_0 is the initial absorbance at frequency v, d is the optical path length in [cm], and I is the irradiance of the laser beam in (W/cm^2). For the calculation of $c(\Gamma_h)$ we use an effective line width $\Gamma_h = 50$ MHz together with the experimental profile of the inhomogeneously broadened absorption band and the chromium(III) concentration of ca. 1.7×10^{-5} mol/cm^3.

$$\phi = \frac{N_A c(\Gamma_h) d(\mathrm{d}A/A_0 \mathrm{d}t)}{(I/hv)(1-10^{-A})}. \quad (1)$$

Using experimental parameters and the data shown in Fig. 4 we derive initial quantum efficiencies of $\approx 9 \times 10^{-7}$ and $\approx 1 \times 10^{-3}$ for the perprotonated and the 50% deuterated crystal, respectively. Hence the quantum efficiency for the hole-burning process increases by approximately three orders of magnitude upon partial deuteration.

In many hydrogen-bonded systems the hole-burning efficiency decreases upon deuteration, and this has been interpreted in terms of the lower tunnelling rate of the deuteron in a double well potential of the hydrogen bond using Gamov's equation for the tunnelling parameter λ [1]:

$$\lambda = \sqrt{2mV}\frac{d}{\hbar}. \quad (2)$$

In Eq. (2) m is the mass of the particle, V is the potential barrier, and d is the distance of the tunnelling. According to this equation the tunnelling parameter should increase by approximately square root of two upon deuteration. The tunnelling frequency is given by Eq. (3)

$$W = \omega_0 \exp(-\lambda). \quad (3)$$

Since the relaxation rate between two wells is proportional to the square of W, a massive *decrease* of the tunnelling rate is expected, and usually observed, upon deuteration. For example, this has been reported for aluminium phthalocyanine tetrasulfonate in hyperquenched glassy films of water where a *reduction* of the quantum yield of >500 was observed [17].

The present system shows the opposite effect and hence cannot be accounted for by the standard tunneling model. It is well documented that water molecules of crystallization can undergo rapid 180° flip motions at room temperature and activation barriers of 10–60 kJ/mol have been measured by solid state NMR spectroscopy [18,19]. The 180° flip motion may thus provide an explanation for the enormous increase in the hole-burning efficiency and the appearance of sharp anti-holes upon partial deuteration. The protonated system is nominally in an identical state after each flip. Hence hole-burning will only occur if the flip is not perfect and the system is slightly disturbed. For example, the water molecule may end up in a slightly altered position. It is also possible that in this case some of the hole-burning is based on the standard translational tunnelling of the proton in the double well potential of the hydrogen bond. In contrast, if a DHO molecule flips, the total zero-point energies of the excited and ground of the chromophore change because the two hydrogen atoms of the water molecules are crystallographically inequivalent (see description of hydrogen bonding above). The change of the zero-point energy is different for the excited and ground state and hence the energy of the zero-phonon line changes. Thus each photoinduced flip of a DHO molecule is accompanied by spectral hole-burning. Support for this interpretation stems from following arguments:

(1) The energies of the anti-holes are very well defined. Since all oxygen atoms of the oxalate ligands are crystallographically inequivalent and the O..O distance of the oxygen atoms involved in hydrogen bonding varies from 2.72 to 2.96 Å distinct sharp anti-holes can be expected upon the flip of DHO molecules.

(2) The anti-holes are symmetrically arranged, indicating that the system does not equilibrate to a particular configuration at low temperature. This is at variance with a hole-burning mechanism based on the translation of hydrogen in an asymmetric double well potential. In this latter picture the 'photoproduct' would occur preferentially on one side.

(3) Hole-burning curves clearly support the proposed mechanism. The efficiency is high when

there is a maximum of DHO molecules in the surroundings of $[Cr(oxalate)_3]^{3-}$. For the fully deuterated crystal (deuteration degree ≈99%) the efficiency is only high for the initial 20% of the hole depth. The remaining 80% show a hole-burning efficiency that is comparable with the one of the perprotonated crystal. Statistically, about 83% of the complexes will have all nine water molecules deuterated in a 99% deuterated crystal. Another confirmation stems from the nominally perprotonated sample. The initial 0.5% hole depth shows a much higher quantum efficiency. This is due to the presence of DHO molecules by the naturally occurring deuterium (0.015%): 0.27% of the complexes will have at least one DHO species amongst the nine water molecules.

4. Conclusions

Partial deuteration of lattice water molecules results in a dramatic increase of the hole-burning efficiency in the R_1-line of $NaMgAl(oxalate)_3 \cdot 9H_2O$:Cr(III) and extremely sharp anti-holes are observed. The results cannot be explained in the standard picture of proton/deuteron tunnelling in a double well of a hydrogen bond and we conclude that the hole-burning mechanism is based on the rotational reorientation of water molecules of crystallization around their pseudo C_2 axes. When the DHO molecules undergo a 180° flip motion the difference in the zero-point energies of the excited and ground state, and hence the transition frequency, changes. This efficient spectral hole-burning mechanism may occur in many other (related) systems. We note here that the present work is somewhat related to the beautiful infrared hole-burning experiments on N-D and O-D stretch bands by Strauss et al. [20].

Since the deuteration also increases the thermal barrier for spontaneous hole-filling from ca. 50 K to ca. 100 K in the present system, it may be possible to design materials for applications in frequency or time domain optical storage at liquid nitrogen temperatures, in frequency stabilization schemes and in frequency standards.

Acknowledgements

This work was supported by the Australian Research Council (large grant no A00104371).

References

[1] W.E. Moerner (Ed.), Persistent Spectral Hole-Burning: Science and Applications, Topics in Current Physics, vol. 44, Springer, Berlin, 1988.
[2] R. Jankowiak, J.M. Hayes, G.J. Small, Chem. Rev. 93 (1993) 1471.
[3] T. Reinot, V. Zazubovich, J.M. Hayes, G.J. Small, J. Phys. Chem. B 105 (2001) 5083.
[4] G.K. Liu, S.T. Li, J.V. Beitz, J. Lumin. 83–84 (1999) 343.
[5] K. Holliday, N.B. Manson, J. Phys.: Condens. Matter 1 (1989) 1339.
[6] R.J. Reeves, R.M. Macfarlane, J. Opt. Soc. Am. B 9 (1992) 763.
[7] R.M. Macfarlane, R.J. Reeves, G.D. Jones, Opt. Lett. 12 (1987) 660.
[8] H. Riesen, V.E. Bursian, N.B. Manson, J. Lumin. 85 (1999) 107.
[9] M.L. Lewis, H. Riesen, J. Phys. Chem. A 106 (2002) 8039.
[10] J.L. Hughes, H. Riesen, J. Phys. Chem. A 107 (2003) 35.
[11] H. Riesen, J.L. Hughes, Chem. Phys. Lett. 370 (2003) 26.
[12] O.S. Mortensen, J. Chem. Phys. 47 (1967) 4215.
[13] J.-S. Suh, J.-Y. Shin, C. Yoon, K.-W. Lee, I.-H. Suh, J.-H. Lee, B.-Y. Ryu, S.-S. Lim, Bull. Korean Chem. Soc. 15 (1994) 245.
[14] A.D. Rae, H. Riesen, to be published.
[15] T.S. Piper, R.L. Carlin, J. Chem. Phys. 35 (1961) 1809.
[16] L. Frossard, Schweiz. Mineral. Petrog. Mitt. 36 (1956) 1.
[17] W.-H. Kim, T. Reinot, J.M. Hayes, G.J. Small, J. Chem. Phys. 104 (1996) 6415.
[18] K. Larsson, J. Tegenfeldt, J. Mol. Struct. 178 (1988) 351.
[19] M. Mizuno, Y. Hamada, T. Kiahara, M. Suhara, J. Phys. Chem. A 103 (1999) 4981.
[20] Y.-H. Cha, H.L. Strauss, J. Phys. Chem. A 106 (2002) 3531, and references [10–12] therein.